



This discussion paper is/has been under review for the journal Atmospheric Measurement Techniques (AMT). Please refer to the corresponding final paper in AMT if available.

Parameterizing radiative transfer to convert MAX-DOAS dSCDs into near-surface box averaged mixing ratios and vertical profiles

R. Sinreich¹, A. Merten^{2,*}, L. Molina³, and R. Volkamer^{1,4}

¹Department of Chemistry and Biochemistry, University of Colorado at Boulder, Colorado, USA

²Institute for Environmental Physics, University of Heidelberg, Heidelberg, Germany

³Molina Center for Energy and the Environment, La Jolla, CA, USA

⁴Cooperative Institute for Research in the Environmental Studies, Boulder, Colorado, USA

* now at: Fraunhofer-Institut für Photonische Mikrosysteme, Dresden, Germany

Received: 31 July 2012 – Accepted: 10 October 2012 – Published: 18 October 2012

Correspondence to: R. Volkamer (rainer.volkamer@colorado.edu)

Published by Copernicus Publications on behalf of the European Geosciences Union.

AMTD

5, 7641–7673, 2012

Discussion Paper | Discussion Paper

Parameterizing
radiative transfer

R. Sinreich et al.

Title Page

Abstract

Introduction

Conclusions

References

Tables

Figures

◀

▶

◀

▶

Back

Close

Full Screen / Esc

Printer-friendly Version

Interactive Discussion



Abstract

We present a novel parameterization method to convert Multi-Axis Differential Optical Absorption Spectroscopy (MAX-DOAS) differential Slant Column Densities (dSCDs) into near-surface box averaged volume mixing ratios. The approach is applicable inside the planetary boundary layer under conditions with significant aerosol load, does not require a-priori assumptions about the trace gas vertical distribution and builds on the increased sensitivity of MAX-DOAS near the instrument altitude. It parameterizes radiative transfer model calculations and significantly reduces the computational effort. The biggest benefit of this method is that the retrieval of an aerosol profile, which usually is necessary for deriving a trace gas concentration from MAX-DOAS dSCDs, is not needed.

The method is applied to NO₂ MAX-DOAS dSCDs recorded during the Mexico City Metropolitan Area 2006 (MCMA-2006) measurement campaign. The retrieved volume mixing ratios of two elevation angles (1° and 3°) are compared to volume mixing ratios measured by two long-path (LP)-DOAS instruments located at the same site. Measurements are found to agree well during times when vertical mixing is expected to be strong. However, inhomogeneities in the air mass above Mexico City can be detected by exploiting the different horizontal and vertical dimensions probed by MAX-DOAS measurements at different elevation angles, and by LP-DOAS. In particular, a vertical gradient in NO₂ close to the ground can be observed in the afternoon, and is attributed to reduced mixing coupled with near surface emission. The existence of a vertical gradient in the lower 250 m during parts of the day shows the general challenge of sampling the boundary layer in a representative way and emphasizes the need of vertically resolved measurements.

Parameterizing radiative transfer

R. Sinreich et al.

Title Page

Abstract	Introduction
Conclusions	References
Tables	Figures

|◀ |▶|
◀ ▶
Back Close
Full Screen / Esc

Printer-friendly Version



1 Introduction

There are different ways to measure trace gases in the atmosphere. In-situ techniques detect very localized trace gas information, and are able to resolve concentration gradients in plumes as air masses move across the instrument inlet. Such measurements

- 5 face a challenge, which consists in how to assess representative concentrations over extended spatial scales as they are being predicted by atmospheric models and measured by satellites. In contrast, Multi Axis Differential Optical Absorption Spectroscopy (MAX-DOAS) measurements integrate over a long distance and measure trace gases through the whole atmosphere (Hönninger and Platt, 2002), which inherently averages
- 10 trace gas inhomogeneities. MAX-DOAS is an application of the well established DOAS technique. DOAS uses the wavelength position and optical density of narrow band absorption features (< 5 nm width) to selectively detect and quantify trace gases by applying Lambert-Beer law (Platt, 1994; Platt and Stutz, 2008). In particular, MAX-DOAS uses scattered sunlight observed from multiple viewing directions, which increases the
- 15 sensitivity to trace gases close to the surface due to differences in the respective light path distributions; i.e. in general, a lower “elevation angle” leads to longer light paths through a trace gas layer near the instrument altitude and thus to a stronger absorption signal (elevation angle is defined as the angle between the horizontal and the pointing direction of the telescope) (e.g. Hönninger and Platt, 2002; van Roozendael et al., 2003; Hönninger et al., 2004; Wagner et al., 2004). However, the presence of aerosols
- 20 in the atmosphere can shorten (or also lengthen) these light paths. The primary quantity of DOAS measurements is the differential Slant Column Density (dSCD), which is the difference of integrated concentrations along the averaged light path of a measurement with low elevation angle and one of a reference (typically from the zenith). The
- 25 light path distribution (different photon paths from the sun through the atmosphere to the collecting telescope) of MAX-DOAS measurements is initially not known, and can be simulated with radiative transfer models. Since the dSCD value depends on the light path through the absorber layer the knowledge of the aerosol profile, in general, is

Parameterizing radiative transfer

R. Sinreich et al.

[Title Page](#)

[Abstract](#)

[Introduction](#)

[Conclusions](#)

[References](#)

[Tables](#)

[Figures](#)

[|◀](#)

[▶|](#)

[◀](#)

[▶](#)

[Back](#)

[Close](#)

[Full Screen / Esc](#)

[Printer-friendly Version](#)

[Interactive Discussion](#)



a prerequisite for the retrieval of a trace gas concentration from MAX-DOAS measurements. In contrast, Long Path DOAS (LP-DOAS) uses an artificial light source whose light is typically retro-reflected in a distance (typically up to 15 km) and collected with a telescope at the place of the light source. Thus, for LP-DOAS the light path is given

5 by twice the distance of telescope/light source and retro-reflector and therefore well defined. The LP-DOAS light beam is usually close to the surface (ca. 1–100 m average height) (e.g. Wang et al., 2006) and cannot be used to derive information from higher altitudes. It is still sensitive to local emissions, however horizontal concentration gradients are inherently averaged over the light beam distance. While in theory, LP-DOAS
10 can realize longer light paths close to the surface than MAX-DOAS (Stutz and Platt, 2008), limitations exist in the available line of sights due to the need to find appropriate places for the setup of retro-reflectors.

The conversion of MAX-DOAS dSCDs into concentrations or volume mixing ratios (VMRs) can be a challenge since the photon light paths through the atmosphere from the sun to the MAX-DOAS device are unknown. The easiest approach is the geometric approximation introduced by Hönniger and Platt (2002). However, it does not account for aerosols in the atmosphere, which can significantly influence the light paths. Approaches which consider aerosols are two step techniques and use radiative transfer modeling (RTM), which simulates photon light paths through the atmosphere. First, the aerosol profile is derived which, then in a second step, is used to determine the trace gas profile. This has been done using optimal estimation (Rodgers, 2000; applied by e.g. Irie et al., 2008; Inomata et al., 2008; Clemer et al., 2010), which needs a-priori assumptions and can use several wavelengths for enhancing the information content of the measurement. A similar method is the regularization (Steck, 2002; applied by Prados-Roman et al., 2011). However, both methods need relatively high computational effort. Trace gas profile retrievals have also be performed by manual iteration until the RTM results match the measurement (e.g. Heckel et al., 2005). Simpler methods make certain presumptions about the profile, e.g. the height of a layer or the shape of a profile, and focus on a few key parameters (e.g. Wittrock et al., 2004;

Parameterizing radiative transfer

R. Sinreich et al.

Title Page

Abstract	Introduction
Conclusions	References
Tables	Figures

A set of four blue rectangular buttons arranged in a 2x2 grid. The top row contains a left arrow button on the left and a right arrow button on the right. The bottom row contains a back button on the left and a close button on the right. Below the grid is a label "Full Screen / Esc".

Printer-friendly Version



Parameterizing radiative transfer

R. Sinreich et al.

Sinreich et al., 2005; Wagner et al., 2011) which gives coarser profiles but relative good VMR/concentration results. Here we present a new method to convert MAX-DOAS dSCDs into near-surface box averaged VMRs in the lowest layer(s) of the planetary boundary layer (PBL). It is a one-step method and is applicable in cases when aerosols constrain the light path in a trace gas layer. Then, the differential light path (path difference between low elevation angle and a reference with a high elevation angle) is determined, which is used to derive the trace gas VMR. Although, with this method, radiative transfer calculations are performed the computational effort is less compared to optimal estimation profile calculations or regularization. It also needs only one wavelength (for O₄) to derive the differential light path distribution, which is useful in cases when the spectral range of the spectrometer is limited to only one O₄ absorption band, and moderately high aerosol load typical of the marine boundary layer and in megacities is present. Since the MAX-DOAS technique loses sensitivity at higher altitudes (averaging kernels of current inverse approaches decrease rapidly above 1km altitude) the derived near-surface box VMRs can be used for a priori estimates of more complex profile retrievals to increase computational efficiency and provide high resolved near-surface vertical profiles depending on the elevation angles used in the measurement.

In the following Sect. 2 the parameterization method is described. In Sect. 3, it is applied to MAX-DOAS dSCD measurements of NO₂ during the Mexico City Metropolitan Area 2006 (MCMA-2006) measurement campaign. The hereby derived VMRs derived from MAX-DOAS measurements pointing into three different directions are compared with LP-DOAS measurements (Merten, 2008) in two (nearly opposite) horizontal directions at roof top level.

2 Description of the parameterization method

MAX-DOAS performed from the ground uses the general rule that the lower the elevation angle the higher is the absorption signal for a trace gas layer located close to ground. However, the presence of an elevated aerosol load in the lowest atmospheric

7645

Title Page

Abstract

Introduction

Conclusions

References

Tables

Figures

1

A small white triangle pointing right, indicating the next slide in a presentation.

Back

Close

Full Screen / Esc

Interactive Discussion



**Parameterizing
radiative transfer**

R. Sinreich et al.

layer shortens the light paths. This can happen to the extent that the light path lengths of the lowest elevation angles do not distinguish significantly from that of a nearby elevation angle. This incidence can be used to derive near-surface box averaged VMRs as shown in this paper, which often happens in a polluted environment or even in the marine boundary layer. Then it can be observed that pointing below a certain elevation angle yields dSCD values that are essentially indistinguishable from each other and independent of the choice of the (low) elevation angle (within the analysis error). Figure 1 illustrates such a scenario in a simplified single-scattering case, but the concept is also valid for multi-scattering cases. Sunlight (yellow arrows) is reaching the atmosphere under a solar zenith angle ϑ . In the atmosphere, it is scattered (indicated by red dots) either above or inside an absorber layer (light blue) located in the PBL close to the ground, depending on the elevation angle of the measurement device. On the right hand side, the corresponding height concentration profile of the absorber is plotted in pink. In this sketch, for the lowest three elevation angles, the aerosol load is high enough so that the differences in the path lengths, which usually arise within different elevation angles, are no longer observable. Thus, the effective distance from the scattering events (red dots) to the telescope is about the same. In the lower part of Fig. 1 the photon scattering probability versus the distance from the telescope is qualitatively plotted in purple (Sinreich, 2008) (dotted line connecting the light path of the lowest elevation angle with the scattering probability). The vertical splitting of the light paths of the lowest elevation angles is exaggerated in this drawing for conceptual clarity and, under the atmospheric condition of an elevated aerosol load, plays a minor role compared to the distance of the effective scattering events to the telescope. Then, the light path length from the sun to the effective height of the scattering events of a low elevation angle is almost as long as the one for a reference spectrum to the same height (especially if the reference is acquired close in time to the measurement spectrum) and mainly cancels out applying the DOAS method resulting in differential effective path lengths. The box-averaged concentration c_{avg} relates to the dSCD as follows, which is valid also for an inhomogeneous vertical profile (see also Fig. 2):

Title Page	
Abstract	Introduction
Conclusions	References
Tables	Figures
◀	▶
◀	▶
Back	Close
Full Screen / Esc	
Printer-friendly Version	
Interactive Discussion	



$$\text{dSCD} = \sum_i c_{\text{avg}_i} \cdot \text{d}l_i = c_{\text{avg}} \cdot \text{d}L_{\text{eff}} \quad (1)$$

with dSCD as the dSCD for the absorber, c_{avg_i} as the mean concentration of the absorber along the differential path with the length, on which photon i travels, and $\text{d}L_{\text{eff}}$ as the differential effective path length of a measurement. The light path of the higher elevation angle plotted in Fig. 1 shows that with increasing elevation angle a point is reached where the light path is less constrained by the presence of aerosols.

A tracer for the light path distribution can be found in the absorption of the trace gas O_4 (e.g. Wagner et al., 2004; Sinreich et al., 2005; Frieß et al., 2006). The concentration of the oxygen dimer O_4 is proportional to the concentration of O_2 squared (Greenblatt et al., 1990, Volkamer, 1996). Thus, the concentration profile shape is well known and is quantitatively dependent only on the air density. Changes in the dSCDs of O_4 indicate changes in the state of the atmosphere (i.e. mainly aerosol load) and measurement geometry (i.e. elevation angle, relative azimuth angle to the sun and solar zenith angle), respectively.

In cases in which the O_4 dSCDs of the lowest elevation angles are the same (referred to as collapsing of the dSCDs in the further text) the O_4 dSCD can be used to determine the effective light path length in the PBL to the telescope. This path length then allows the calculation of the near-surface box averaged VMR of the trace gas of interest according to Eq. (1). As illustrated in Fig. 2 with NO_2 as example for the trace gas of interest the dSCDs (of a low elevation angle) of O_4 and NO_2 are the inputs from the measurement (left hand side). The collapsing of the O_4 dSCDs of the lowest elevations angles to a single value within the analysis error is a prerequisite for applying this method since this ensures that the scattering events happened at comparable distances. Thus, when applying it to measurement data an according filtering is performed before further processing the data. Then the NO_2 dSCDs collapse as well if the NO_2 layer can be approximated to a homogeneous near surface layer (yielding an average box profile concentration or VMR value). By dividing the filtered O_4 dSCD by the typical

Parameterizing radiative transfer

R. Sinreich et al.

[Title Page](#)

[Abstract](#)

[Introduction](#)

[Conclusions](#)

[References](#)

[Tables](#)

[Figures](#)

[◀](#)

[▶](#)

[◀](#)

[▶](#)

[Back](#)

[Close](#)

[Full Screen / Esc](#)

[Printer-friendly Version](#)

[Interactive Discussion](#)



O_4 concentration at instrument altitude ($c_{O_4 \text{instr}}$) a differential O_4 equivalent path length L_{eq, O_4} is calculated:

$$L_{\text{eq}} = \frac{d\text{SCD}_{O_4}}{c_{O_4 \text{instr}}} \quad (2)$$

Here it is assumed that the O_4 concentration does not change significantly between the altitude of the instrument and the effective scattering event. The differential O_4 equivalent path length is the light path length from the effective scattering event to the telescope if O_4 and the trace gas (NO_2) had the same concentration profile shape (here a box profile), which typically is not the case. In a next step, radiative transfer modeling is performed in order to calculate a correction factor which accounts for the different vertical profile shapes of the exponentially decreasing O_4 concentrations with height and the approximated homogenous layer for NO_2 (Volkamer et al., 2009). In addition, the correction factor can account for different absorbing wavelengths of the two gases. Multiplication of the differential O_4 equivalent path length with the correction factor yields the differential effective path length. Dividing the NO_2 dSCD by the differential NO_2 effective path length leads to the average NO_2 concentration or VMR in a box that reaches from the ground to height h_{eff} :

$$h_{\text{eff}} = dL_{\text{eff}} \cdot \tan \alpha \quad (3)$$

with α as the elevation angle.

The correction factor is not a constant. In general, it depends on any factor of the state of the atmosphere (aerosol optical density, PBL height etc.) and of the measurement geometry (solar zenith angle, elevation angle etc.), respectively. Figure 3 shows calculated correction factors from 3° elevation angle data for 4 O_4 absorption bands: 360 nm, 477 nm, 577 nm and 630 nm. In the upper panel (Fig. 3a–d) the correction factors are plotted as a function of aerosol optical density (AOD) for different elevation angles for arbitrarily picked scenarios which cover mostly the range of investigated absorbing wavelength, SZA and PBL height: (a) 360 nm, 10° SZA and 0.5 km PBL height;

Parameterizing radiative transfer

R. Sinreich et al.

[Title Page](#)

[Abstract](#)

[Introduction](#)

[Conclusions](#)

[References](#)

[Tables](#)

[Figures](#)

[|◀](#)

[▶|](#)

[◀](#)

[▶](#)

[Back](#)

[Close](#)

[Full Screen / Esc](#)

[Printer-friendly Version](#)

[Interactive Discussion](#)



(b) 477 nm, 30° SZA and 1 km PBL height; (c) 577 nm, 50° SZA and 1 km PBL height; (d) 630 nm, 70° SZA and 2 km PBL height. For the underlying radiative transfer calculations the trace gas profile has been chosen as a box profile with a constant mixing ratio in the PBL, though this is not a requirement for the approach. The trace gas is a weak absorber and absorbs at the O₄ wavelengths. The elevation angles are 1°, 3°, 6°, 10°, 20° and zenith, and the solar relative azimuth angle (i.e. the horizontal projection of the angle between sun and the measurement viewing direction, SRAA) is always 90°. The asymmetry parameter (g) of the aerosol layer in the PBL has been chosen to be 0.68, which is a typical value for urban aerosols. The single scattering albedo (SSA) is 0.78 for 360 nm and 0.95 for the other wavelengths (see sensitivity studies in Sect. 3). Also, the surface albedo has wavelength dependent values: 0.09 (360 nm), 0.13 (470 nm), 0.17 (577 nm) and 0.2 (630 nm) (Barnard et al., 2008).

The correction factors in Fig. 3 reflect to some extent the behavior of the dSCDs. The split of all elevation angles is only observed under pristine conditions and beginning with a certain AOD aerosol forces the convergence starting with the lowest elevation angles (considering a typical DOAS fit error of 10 %). This means that the collapsing of the dSCDs of the lowest elevation angles can be seen in the correction factors when the AOD reaches a certain value, and the collapsing with even higher elevation angles happens with higher AOD values reflecting further reduced differential path lengths. It is also observable that in the range of collapsing the actual correction factor does not change much in value and shows a kind of plateau. This means that once convergence is observed a further increase in aerosols has limited effect and the effective path length scales linearly with the observed O₄ dSCD. This is of big importance since, in general, the aerosol load is an important limiting factor for the interpretation of MAX-DOAS measurements.

This general behavior of the correction factors can be seen in all investigated wavelengths, layer heights and different solar zenith angles, and also in other studies (Volkanmer et al., 2009; Sinreich et al., 2010).

Parameterizing radiative transfer

R. Sinreich et al.

[Title Page](#)

[Abstract](#)

[Introduction](#)

[Conclusions](#)

[References](#)

[Tables](#)

[Figures](#)

[|◀](#)

[▶|](#)

[◀](#)

[▶](#)

[Back](#)

[Close](#)

[Full Screen / Esc](#)

[Printer-friendly Version](#)

[Interactive Discussion](#)



**Parameterizing
radiative transfer**

R. Sinreich et al.

In a next step, the mean values of the plateaus of each scenario are derived and taken as the corresponding correction factors (and applied to the MAX-DOAS dSCDs later). A range of 0.3 to 0.6 AOD was chosen to determine the mean values. It is useful to set also an upper limit of the AOD because due to applying ratios of differential values the noise in the RTM calculation overlaying the correction factors increases with increasing AOD. Additionally, in some cases a small slope even in the plateau range could be observed, which could be due to multiple scattering in the lowest layer. Thus unrealistically high AOD values should not be considered in this method.

As mentioned above, the trace gas of interest does not need to be well mixed in PBL 10 as long as the aerosol layer is so. The trace gas VMR value is then an average value up to the height of the differential effective scattering event not resolving vertical gradients. In order to illustrate this, a non box profile for the trace gas is considered (the aerosol layer was still a box profile) which is a profile with a constantly decreasing mixing ratio up to top of the PBL where it is zero. Since this triangle shape inherently produces 15 a splitting of the dSCDs on top of the regular MAX-DOAS splitting a higher AOD value range is necessary (0.5–0.8) to observe convergence of the correction factors in the lower elevation angles. Then the correction factors (of 1° and 3°) collapse (within a 10 % error) and it can be approximated to extract box averaged VMRs.

Figure 3e–h shows the mean values of each plateau for different layer heights plotted 20 versus the solar zenith angle (SZA) for the 4 wavelengths. The thick lines are calculated for constant trace gas mixing ratios up to the corresponding height (box profile), thin lines indicate constantly decreasing mixing ratios up to the corresponding height (triangular profile). The errors represent the statistical error, i.e. the standard deviation within the plateaus. In order to create a diurnal plot the morning values of the 25 solar zenith angle are negative. Yet, the values are symmetric towards 0° SZA showing “tooth-shapes” (caused by the pronounced forward scattering on aerosols in the zenith reference). This symmetry is owing to the constant azimuth angle, and as shown in Sect. 3.1 the plot can become significantly asymmetric with changing azimuth angle (or changing layer height or both). In these figures it can be seen that, for most SZA,

Title Page	
Abstract	Introduction
Conclusions	References
Tables	Figures
◀	▶
◀	▶
Back	Close
Full Screen / Esc	
Printer-friendly Version	
Interactive Discussion	



**Parameterizing
radiative transfer**

R. Sinreich et al.

[Title Page](#)[Abstract](#)[Introduction](#)[Conclusions](#)[References](#)[Tables](#)[Figures](#)[|◀](#)[▶|](#)[◀](#)[▶](#)[Back](#)[Close](#)[Full Screen / Esc](#)[Printer-friendly Version](#)[Interactive Discussion](#)

3 MCMA-2006 case study

3.1 Correction factors for the MCMA-2006 MAX-DOAS setup

The correction factors in this section are calculated for the example of Mexico City, which is located at about 2200 m a.s.l. In 2006, during the MCMA-2006 measurement campaign MAX-DOAS measurements were performed at the “T0 site” in about 15 m height on the roof top of the Instituto Mexicano del Petroleo (IMP, a 4 level building), which is located at the North edge of Mexico City downtown. The retrieved dSCDs of NO₂ and O₄ are applied to the parameterization method. For the calculation of the correction factors, we used the radiative transfer model McArtim (Deutschmann, 2009; Deutschmann et al., 2011). The model is initiated using values for surface albedo (0.09), single scattering albedo (0.78), and asymmetry parameter (0.68) as measured for urban pollution in Mexico City (Barnard et al., 2008). The O₄ dSCD is retrieved from the 360 nm absorption band and the NO₂ dSCD from a DOAS fitting in wavelength range between 368 nm and 390 nm.

For the example of the MCMA-2006 measurements an aerosol optical density between 0.3 and 0.6 is a good range for layer heights from 500 m to 3000 m to reflect the overlapping of the observed 1° and 3° elevation angles. Higher AOD values would lead to an additional collapsing of further (higher) elevation angle values, which was mainly not observed in the measurements. The mean values over this AOD range were used as correction factors which are being applied to the MAX-DOAS dSCDs.

With the radiative transfer parameters mentioned at the beginning of this section, differential air mass factors (dAMFs) for O₄ and NO₂ were simulated. The AMF is the ratio of slant (SCD) and vertical column density (VCD), where the latter one is the integrated concentration over the height. It is a measure for the light path enhancement compared to the vertical path through the atmosphere.

In general, the correction factor f_c is the ratio of the trace gas concentration which is retrieved by radiative transfer calculations ($c_{\text{retrieved}}$) and the trace gas concentration

[Title Page](#)[Abstract](#)[Introduction](#)[Conclusions](#)[References](#)[Tables](#)[Figures](#)[|◀](#)[▶|](#)[◀](#)[▶](#)[Back](#)[Close](#)[Full Screen / Esc](#)[Printer-friendly Version](#)[Interactive Discussion](#)

which is input for these calculations (c_{real}). For the MCMA-2006 MAX-DOAS setup the correction factors are further calculated as follows:

$$f_c = \frac{c_{\text{retrieved}}}{c_{\text{real}}} = \frac{\text{dAMF}_{\text{NO}_2} \cdot \text{PBLh} \cdot c_{\text{O}_4}}{\text{dAMF}_{\text{O}_4} \cdot \text{VCD}_{\text{O}_4}} \quad (4)$$

whereby $\text{dAMF}_{\text{NO}_2}$ and dAMF_{O_4} are the dAMFs for NO_2 and O_4 , calculated from the radiative transfer model McArtim for a specific solar zenith angle, elevation angle, wavelength, NO_2 vertical profile etc., c_{O_4} is a typical surface concentration for O_4 ($1.87 \times 10^{37} \text{ molecules}^2 \text{ cm}^{-6}$), VCD_{O_4} is the corresponding typical VCD for O_4 ($0.90 \times 10^{43} \text{ molecules}^2 \text{ cm}^{-5}$), and PBLh is the assumed PBL height. For this method, it is necessary to know or at least estimate the PBL height. Mexico City is known for its dynamic PBL, and in extreme cases of PBL variability the correction factor can vary by a factor of 3 over the course of a day. As shown in the last section, accurate knowledge of PBL height is more crucial in the morning when the PBL height is lower. Here, a typical diurnal PBL height cycle was estimated to be about 500 m until 09:00 a.m. (local time), then rise up constantly until 2500 m at 03:00 p.m. and stay at this height until the end of the day (see inset of Fig. 5). This is compatible with measurements of the PBL made by de Foy et al. (2005) in MCMA-2003 and by K. Knupp and D. Phillips from The National Space Science and Technology Center of the University of Alabama at Huntsville in MCMA-2006.

For the MCMA-2006 case study, the variability of the correction factor is investigated in some more detail. While this method largely eliminates the sensitivity to the aerosol optical density the sensitivity towards other parameters of the state of the atmosphere and measurement geometry still applies, as seen above for the case of the PBL height. Most important parameters are here SRAA, surface albedo (SA), g and SSA. Table 1 lists the relative change of the correction factor of the three latter parameters for different PBL heights (PBLh) and SZA when applying the corresponding parameter and leave the others at standard values (SA = 0.09; g = 0.68; SSA = 0.78). The error is a statistical error resulting from the standard deviations when retrieving the plateau

[Title Page](#)

[Abstract](#)

[Introduction](#)

[Conclusions](#)

[References](#)

[Tables](#)

[Figures](#)

[|◀](#)

[▶|](#)

[◀](#)

[▶](#)

[Back](#)

[Close](#)

[Full Screen / Esc](#)

[Printer-friendly Version](#)

[Interactive Discussion](#)



Parameterizing radiative transfer

R. Sinreich et al.

[Title Page](#)

[Abstract](#)

[Introduction](#)

[Conclusions](#)

[References](#)

[Tables](#)

[Figures](#)

[|◀](#)

[▶|](#)

[◀](#)

[▶](#)

[Back](#)

[Close](#)

[Full Screen / Esc](#)

[Printer-friendly Version](#)

[Interactive Discussion](#)



values. The SRAA, which is important since aerosols scatter light preferably in forward direction, is investigated separately further below.

As can be seen all virtual changes are below 10 %, and thus only play a minor role for the derivation of the mixing ratios. An exception is the asymmetry parameter for low layer heights for which changes are smaller than 15 %.

The dependence of the correction factor on the SRAA was considered for the MCMA-2006 MAX-DOAS setup specifically. The MAX-DOAS measurements collected light simultaneously from the North, West and South (about 7° rotated clockwise to the exact geographical directions). The radiative transfer calculations were made with the corresponding RSAA depending on the time of the day. The correction factors considering azimuth effect and diurnal PBL dynamics are plotted in Fig. 5. No measurements were performed in East direction and calculations in East direction are added here to demonstrate the azimuth effect. While in the afternoon the correction factors of all 4 directions in Fig. 5 are very similar, they show significant differences when PBL and SRAA are low (East and South in the morning). The North and West direction values show a morning increase (also due to the expansion of the PBL) which is hardly affected by an azimuth effect. Figure 5 shows that a small SRAA (< 50°) has a larger effect on the correction factors the lower the PBL is. This is qualitatively consistent with the g dependence on the PBL height shown in Table 1.

20 3.2 Determination of MAX-DOAS VMRs and comparison with LP-DOAS during MCMA-2006

The correction factors f_c from Fig. 5 were used to convert the NO₂ dSCDs (dSCD_{NO₂}) into mixing ratios VMR_{NO₂} by means of corresponding O₄ dSCDs (dSCD_{O₄}) using 1° and 3° elevation angle:

$$25 \text{ VMR}_{\text{NO}_2} = \frac{1}{f_c} \cdot \frac{\text{dSCD}_{\text{NO}_2} \cdot c_{\text{O}_4}}{\text{dSCD}_{\text{O}_4}} \cdot \frac{1}{m} \quad (5)$$

with m as the conversion factor from concentration to VMR ($m = 2.0 \times 10^{10} \text{ ppb cm}^{-3} \text{ molecules}^{-1}$, 1 ppb = 1 part per billion).

Figure 6 shows the mixing ratio time series of MAX-DOAS in South direction exemplarily for 3 arbitrary days (23–25 March 2006). There are gaps in the time series when there was no sunlight. Also VMR values of two LP-DOAS measurements from the same site pointing to the South and to the Northwest with retro-reflectors in about 2.6 km and 1 km distance, respectively, are shown (Merten, 2008). During daylight ($\text{SZA} < 90^\circ$, light yellow background in Fig. 6) a general agreement in the shape can be seen. However, for MAX-DOAS the peak on 23 March is not as high as for LP-DOAS and on 24 March some scatter can be seen for both MAX-DOAS and the two LP-DOAS. Also, differences between the two LP-DOAS are observable several times indicating horizontal inhomogeneities.

In order to assess the diurnal behavior for the overall time series, in the following, half-hourly medians are taken for the time when all three instruments conducted measurements (10 March–1 April 2006). Figure 7 compares the mixing ratios of MAX-DOAS of all directions and of LP-DOAS of both directions each for 1° (upper panel) and 3° (lower panel). The values are plotted as whiskers with crosses indicating medians and vertical extensions the 25 %-tiles and 75 %-tiles of the values. The MAX-DOAS whiskers represent the statistics from all three viewing directions. Additionally the values of the individual MAX-DOAS directions are plotted as lines, which show a small horizontal variability only between 10:30 a.m. and 12:30 p.m. in both 1° and 3° . For the rest of the median diurnal profile the values of the 3 directions lie mainly on top of each other, which is a confirmation of the calculated azimuth effect shown in Fig. 5. In general, the MAX-DOAS and LP-DOAS values show good agreement. However, the LP-DOAS has significant higher values than MAX-DOAS in the afternoon, when the mixing in the PBL is less active and O_3 concentrations are typically high (Volkamer et al., 2010). This is slightly more pronounced in the case of 3° elevation angle than in 1° elevation angle, which indicates a vertical gradient. Also the values of the two LP-DOAS directions lie on top of each other except for the time between 09:00 a.m.

[Title Page](#)[Abstract](#)[Introduction](#)[Conclusions](#)[References](#)[Tables](#)[Figures](#)[|◀](#)[▶|](#)[◀](#)[▶](#)[Back](#)[Close](#)[Full Screen / Esc](#)[Printer-friendly Version](#)[Interactive Discussion](#)

Parameterizing radiative transfer

R. Sinreich et al.

and 11:00 a.m. where the Northwest direction show almost up to double as much NO₂ as the South direction. It is surprising that the values of the 2 LP-DOAS directions temporarily differ by a factor of 2 although the MAX-DOAS values of the three directions mostly agree with each other. Despite the relatively strong scatter in the LP-DOAS 5 values it indicates that there are horizontal gradients which are not detected by MAX-DOAS. Hence, it must only happen below the MAX-DOAS line of sight of 1° elevation angle, hence in the lowest couple of 10 meters (see Sect. 3.3).

In Fig. 8 the horizontal (left panel) and vertical (right panel) extent of the air masses probed by the MAX-DOAS measurements for 1° (upper panel) and 3° (lower panel) elevation angle is plotted. This is the differential effective path length and its vertical projection (see Eq. 3), which represents the spatial fetch of the MAX-DOAS measurements. The horizontal lines indicate the distances from the light source to the respective retro-reflectors for the LP-DOAS measurements. It can be seen in Fig. 8 that until 11:00 a.m. the MAX-DOAS at the measured wavelength and the longer LP-DOAS light path have about the same horizontal expansion. Due to the rising of the PBL and the involved dilution of aerosols the differential effective path length increases continuously over the course of the day and reaches about 2–3 times the horizontal path during afternoons. As expected from the approach description in Chapt. 2, the horizontal path length is comparable for 1° and 3° elevation angle.

20 The same general picture can be observed with the median top height of the differential effective path, h_{eff} , which represents the vertical extent over which the box-averaged VMR is measured. The median day starts with values for h_{eff} around 40 m (1°) and 130 m (3°) vertical dimension increasing during the day to about a factor of 3 to reach about 100 m (1°) and 300 m (3°) in the afternoon. The measurements were
 25 performed on roof-top level so that these heights start at a measurement altitude of about 16 m above ground.

Title Page	
Abstract	Introduction
Conclusions	References
Tables	Figures
◀	▶
◀	▶
Back	Close
Full Screen / Esc	
Printer-friendly Version	
Interactive Discussion	



3.3 Near-surface vertical profile

By combining Fig. 7 with Fig. 8 right panel a near surface vertical profile can be derived. In Fig. 9 this is done for the South direction at a time period from 08:30–09:00 a.m. (red), 12:00–12:30 p.m. (green), and 03:30 to 04:00 p.m. (blue). Especially in the afternoon a significant difference between LP-DOAS and MAX-DOAS is observable. The points at 16 m altitude represent the LP-DOAS data (roof-top altitude). The next higher points are the 1° MAX-DOAS values at half altitude of the effective scattering height. The highest points are retrieved from 3° MAX-DOAS data minus the 1° data, which means that the box-averaged NO₂ VMR for 1° is subtracted from the one for 3°, and this difference is plotted at half height of the difference in 3° and 1° h_{eff} above the 1° layer, i.e. $h_{\text{eff}}(1^\circ) + \frac{h_{\text{eff}}(3^\circ) - h_{\text{eff}}(1^\circ)}{2}$. This ensures that the values in Fig. 9 represent not overlapping layers and that only the mixing ratio retrieved in the respective layer is shown.

Figure 9 shows a dynamic vertical gradient. In the morning, a slight vertical increase in the lowest layer can be seen which turns into a slight decrease at midday. However, both profiles are mostly within the error tolerance. In the afternoon, a significant vertical gradient can be observed, which halves the VMR from 16 m to about 240 m altitude being pronounced towards the ground. A similar vertical gradient has been observed for toluene and C₂-alkylbenzene during MCMA-2003 in Mexico City by Jobson et al. (2010) by a factor of 2 in 21 m difference from the ground. This might indicate that the gradient shown here also continues down to the ground.

Generally, the near-surface vertical profiles are generated by MAX-DOAS and do not need necessarily LP-DOAS values. The vertical spatial resolution depends on the chosen elevation angles steps of the MAX-DOAS measurements and can be relatively high. Also, MAX-DOAS measurements have a high temporal resolution which underlines the importance of MAX-DOAS measurements for the trace gas inventory of a dynamic polluted environment like megacities.

[Title Page](#)[Abstract](#)[Introduction](#)[Conclusions](#)[References](#)[Tables](#)[Figures](#)[|◀](#)[▶|](#)[◀](#)[▶](#)[Back](#)[Close](#)[Full Screen / Esc](#)[Printer-friendly Version](#)[Interactive Discussion](#)

4 Conclusions

A parameterization method to convert MAX-DOAS dSCDs into near-surface box averaged VMRs is described in detail. Differential effective light paths were calculated and correction factors calculated from radiative transfer modeling to derive vertically

5 resolved trace gas mixing ratios. The method is rather insensitive to the assumptions about the state of the atmosphere (aerosol extinction, phase function, surface albedo etc.) if the aerosol load is high enough (typically an aerosol optical density of 0.3 or higher). However, especially the actual trace gas layer height and solar relative azimuth angle (SRAA) have a strong impact in cases when both SRAA and PBL are low.

10 It has in particular several advantages:

1. The approach is straightforward (a one-step conversion) and significantly reduces computational effort.
2. It does not depend on knowing the actual aerosol profile as it is typically necessary for MAX-DOAS concentration retrievals, and can be applied already under conditions of moderately low aerosol load (here AOD ≥ 0.3).
- 15 3. The approach does not suffer from the limited sensitivity of MAX-DOAS at higher altitudes that poses limitations to the use of optimal estimation approaches to infer vertical profiles in situations of high PBL. Yet, this method also can be used as input parameter for more complex retrievals, such as optimal estimation, especially since it provides a reasonably high near-surface vertical resolution (depending on the elevation angle).
- 20 4. It does not require a-priori assumptions about trace gas vertical distributions.
5. It is applicable in cases of limited spectral coverage of the spectrometer (only one O₄ absorption band). Optimal estimation and other retrievals in principle can use only one O₄ band, but face limitations in air masses with high PBL such as Mexico City, where aerosol inferences from use of only one O₄ absorption band

[Title Page](#)

[Abstract](#)

[Introduction](#)

[Conclusions](#)

[References](#)

[Tables](#)

[Figures](#)

[|◀](#)

[▶|](#)

[◀](#)

[▶](#)

[Back](#)

[Close](#)

[Full Screen / Esc](#)

[Printer-friendly Version](#)

[Interactive Discussion](#)



can yield unstable results, but remain pre-requisite to derive trace gas information. Especially if the spectral range does not include the the 477 nm O₄ band or longer wavelengths the information content for aerosol retrievals is relatively limited due to strongly increased scattering at shorter wavelengths.

- 5 During the Mexico City Metropolitan Area 2006 (MCMA-2006) measurement campaign 2 LP-DOAS facing in near opposite directions and a MAX-DOAS pointing in three directions perpendicular to each other were deployed in a systematic effort to access inhomogeneities of the Mexico City air mass. While LP-DOAS averages the trace gas concentration close to the ground with a horizontal expansion of 1 and 2.6 km, respectively,
- 10 MAX-DOAS covers a minimum spatial fetch of 40 m height and 2.5 km horizontal length in the morning (1° elevation angle) up to a maximum of about 350 m height and 5km length in the evening (3°). For the 3° elevation angle data, as expected the vertical extension is about 3 times higher than the one of the 1° elevation angle data. The comparison of the LP-DOAS and MAX-DOAS values gives indication for horizontal and vertical inhomogeneities. In particular, a vertical gradient of NO₂ close to the ground can be concluded in the afternoon. The comparison shows the unique potential
- 15 and importance of MAX-DOAS measurements in polluted dynamic environments like megacities.

20 *Acknowledgements.* Financial support from NSF-SGER (ATM-0827386), NSF-CAREER (ATM-0847793) and CU Boulder startup funds (RV) and MCE2 (LTM) is gratefully acknowledged. Thanks to measurements of PBL in MCMA-2006 made by K. Knupp and D. Phillips from The National Space Science and Technology Center of the University of Alabama at Huntsville. We are also thankful to P. Sheehy for his help performing the LP-DOAS measurements. We thank Gustavo Sosa and local supporters at IMP for the great campaign organization, Ulrich Platt for loan of the instruments, and Thomas Wagner for helpful comments on the manuscript.

25

Parameterizing radiative transfer

R. Sinreich et al.

[Title Page](#)[Abstract](#)[Introduction](#)[Conclusions](#)[References](#)[Tables](#)[Figures](#)[|◀](#)[▶|](#)[◀](#)[▶](#)[Back](#)[Close](#)[Full Screen / Esc](#)[Printer-friendly Version](#)[Interactive Discussion](#)

References

Parameterizing radiative transfer

R. Sinreich et al.

[Title Page](#)

[Abstract](#)

[Introduction](#)

[Conclusions](#)

[References](#)

[Tables](#)

[Figures](#)

◀

▶

◀

▶

[Back](#)

[Close](#)

[Full Screen / Esc](#)

[Printer-friendly Version](#)

[Interactive Discussion](#)



Parameterizing radiative transfer

R. Sinreich et al.

[Title Page](#)

[Abstract](#)

[Introduction](#)

[Conclusions](#)

[References](#)

[Tables](#)

[Figures](#)

[|◀](#)

[▶|](#)

[◀](#)

[▶](#)

[Back](#)

[Close](#)

[Full Screen / Esc](#)

[Printer-friendly Version](#)

[Interactive Discussion](#)



Sinreich, R., Friess, U., Wagner, T., and Platt, U.: Multi axis differential optical absorption spectroscopy (MAX-DOAS) of gas and aerosol distributions, *Faraday Discuss.*, 130, 153–164, doi:10.1039/b419274p, 2005.

Sinreich, R., Coburn, S., Dix, B., and Volkamer, R.: Ship-based detection of glyoxal over the remote tropical Pacific Ocean, *Atmos. Chem. Phys.*, 10, 11359–11371, doi:10.5194/acp-10-11359-2010, 2010.

Steck, T.: Methods for determining regularization for atmospheric retrieval problems, *Appl. Optics*, 41, 1788–1797, 2002.

van Roozendael, M., Fayt, C., Post, P., Hermans, C., Lambert, J.-C.: Retrieval of BrO and NO₂ from UV-visible observations, in: *Sounding the Troposphere from Space: A New Era for Atmospheric Chemistry*, edited by: Borell, P., Borell, P. M., Burrows, J. P., and Platt, U., Springer-Verlag, 2003.

Volkamer, R.: Absorption von Sauerstoff im Herzberg I System und Anwendung auf Aromatenmessungen am European PHOTOREACTOR (EUPHORE), Diploma thesis D-491, University of Heidelberg, Germany, 1996.

Volkamer, R., Coburn, S., Dix, B., and Sinreich, R.: MAX-DOAS observations from ground, ship, and research aircraft: maximizing signal-to-noise to measure “weak” absorbers, *Proc. SPIE*, 7462, 746203, doi:10.1117/12.826792, 2009.

Volkamer, R., Sheehy, P., Molina, L. T., and Molina, M. J.: Oxidative capacity of the Mexico City atmosphere – Part 1: A radical source perspective, *Atmos. Chem. Phys.*, 10, 6969–6991, doi:10.5194/acp-10-6969-2010, 2010.

Wagner, T., Dix, B., v. Friedeburg, C., Friess, U., Sanghavi, S., Sinreich, R., and Platt, U.: MAX-DOAS O₄ measurements: A new technique to derive information on atmospheric aerosols – Principles and information content, *J. Geophys. Res.*, 109, D22205, doi:10.1029/2004JD004904, 2004.

Wagner, T., Beirle, S., Brauers, T., Deutschmann, T., Friess, U., Hak, C., Halla, J. D., Heue, K. P., Junkermann, W., Li, X., Platt, U., and Pundt-Gruber, I.: Inversion of tropospheric profiles of aerosol extinction and HCHO and NO₂ mixing ratios from MAX-DOAS observations in Milano during the summer of 2003 and comparison with independent data sets, *Atmos. Meas. Tech.*, 4, 2685–2715, doi:10.5194/amt-4-2685-2011, 2011.

Parameterizing radiative transfer

R. Sinreich et al.

[Title Page](#)

[Abstract](#)

[Introduction](#)

[Conclusions](#)

[References](#)

[Tables](#)

[Figures](#)

[◀](#)

[▶](#)

[◀](#)

[▶](#)

[Back](#)

[Close](#)

[Full Screen / Esc](#)

[Printer-friendly Version](#)

[Interactive Discussion](#)



Wang, S., Ackermann, R., and Stutz, J.: Vertical profiles of O₃ and NO_x chemistry in the polluted nocturnal boundary layer in Phoenix, AZ: I. Field observations by long-path DOAS, *Atmos. Chem. Phys.*, 6, 2671–2693, doi:10.5194/acp-6-2671-2006, 2006.

5 Wittrock, F., Oetjen, H., Richter, A., Fietkau, S., Medeke, T., Rozanov, A., and Burrows, J. P.: MAX-DOAS measurements of atmospheric trace gases in Ny-Ålesund – Radiative transfer studies and their application, *Atmos. Chem. Phys.*, 4, 955–966, doi:10.5194/acp-4-955-2004, 2004.

**Parameterizing
radiative transfer**

R. Sinreich et al.

[Title Page](#)

[Abstract](#)

[Introduction](#)

[Conclusions](#)

[References](#)

[Tables](#)

[Figures](#)

[|◀](#)

[▶|](#)

[◀](#)

[▶](#)

[Back](#)

[Close](#)

[Full Screen / Esc](#)

[Printer-friendly Version](#)

[Interactive Discussion](#)



Table 1. Correction factor sensitivities to surface albedo (SA), asymmetry parameter g , and single scattering albedo (SSA) when modifying the corresponding parameter (default values: SA = 9 %, g = 0.68, SSA = 0.78)

PBLh (m)	SZA ($^{\circ}$)	SA = 4 %	Sa = 14 %	g = 0.61	g = 0.75	SSA = 0.95
500	20	$-(4.0 \pm 2.2)\%$	$+(3.1 \pm 2.3)\%$	$+(13.3 \pm 3.1)\%$	$-(9.5 \pm 2.1)\%$	$-(0.8 \pm 3.1)\%$
	50	$-(4.8 \pm 3.6)\%$	$+(2.9 \pm 5.2)\%$	$+(7.8 \pm 4.8)\%$	$-(11.2 \pm 5.0)\%$	$+(0.5 \pm 3.4)\%$
	80	$-(0.8 \pm 1.8)\%$	$+(4.0 \pm 3.8)\%$	$+(5.0 \pm 1.6)\%$	$-(3.7 \pm 2.2)\%$	$+(7.7 \pm 2.5)\%$
1000	20	$-(2.9 \pm 1.7)\%$	$+(1.5 \pm 2.4)\%$	$+(7.5 \pm 2.4)\%$	$-(5.3 \pm 1.6)\%$	$-(1.4 \pm 2.2)\%$
	50	$-(3.6 \pm 2.2)\%$	$+(2.8 \pm 1.2)\%$	$+(7.3 \pm 4.0)\%$	$-(4.8 \pm 2.5)\%$	$+(1.4 \pm 2.3)\%$
	80	$-(0.6 \pm 1.1)\%$	$+(0.8 \pm 1.8)\%$	$+(3.1 \pm 2.5)\%$	$-(2.9 \pm 2.0)\%$	$+(4.0 \pm 3.3)\%$
2000	20	$+(0.3 \pm 1.3)\%$	$+(1.9 \pm 1.7)\%$	$+(4.2 \pm 2.2)\%$	$-(1.5 \pm 1.8)\%$	$-(0.1 \pm 1.0)\%$
	50	$-(4.0 \pm 1.5)\%$	$-(1.2 \pm 1.4)\%$	$-(2.1 \pm 2.5)\%$	$-(5.2 \pm 1.8)\%$	$-(1.9 \pm 1.6)\%$
	80	$-(1.0 \pm 1.6)\%$	$+(0.3 \pm 1.3)\%$	$+(0.9 \pm 1.8)\%$	$-(1.8 \pm 2.1)\%$	$+(1.5 \pm 3.1)\%$
3000	20	$-(1.0 \pm 1.4)\%$	$-(0.5 \pm 1.0)\%$	$+(0.7 \pm 0.7)\%$	$-(1.0 \pm 0.3)\%$	$-(1.7 \pm 1.2)\%$
	50	$+(0.9 \pm 0.5)\%$	$+(1.9 \pm 1.8)\%$	$+(1.8 \pm 1.4)\%$	$+(0.8 \pm 2.5)\%$	$+(1.0 \pm 1.2)\%$
	80	$-(0.6 \pm 0.9)\%$	$-(1.1 \pm 0.6)\%$	$-(0.6 \pm 2.2)\%$	$(0.0 \pm 2.1)\%$	$+(0.3 \pm 2.7)\%$

Title Page	Abstract	Introduction
Conclusions	References	
Tables	Figures	
◀	▶	
◀	▶	
Back	Close	
Full Screen / Esc		

Printer-friendly Version
Interactive Discussion



Parameterizing radiative transfer

R. Sinreich et al.

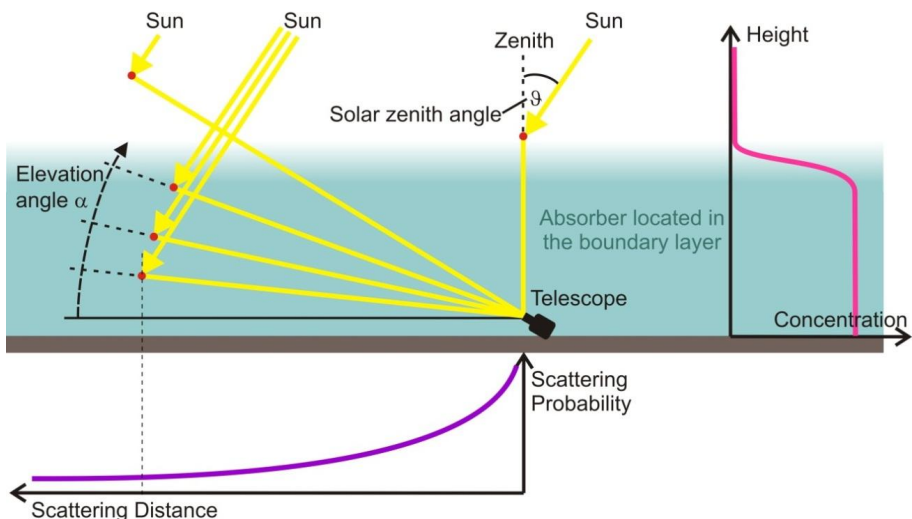


Fig. 1. Sketch of the light paths in a single scattering case when this approach can be applied. Photons coming from the sun are scattered in the atmosphere (red dots) before they reach the MAX-DOAS device. An elevated aerosol load in the lowest atmosphere shortens the light path and can lead to indistinguishable dSCD values for low elevation angles. On the right hand side, the concentration profile of the absorber and, in the lower part, the photon scattering probability versus the distance from the telescope are indicated. For further information see text.

Title Page

Abstract

Introduction

Conclusions

References

Tables

Figures

1

A small blue triangle icon with a white border, positioned at the bottom right corner of the slide.

1

1

Back

Close

Full Screen / Esc

[Printer-friendly Version](#)

Interactive Discussion



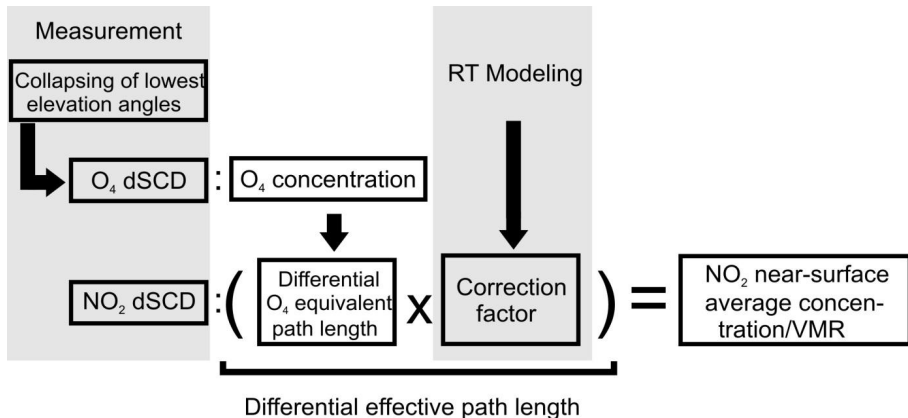


Fig. 2. Retrieval algorithm with NO_2 as example for the trace gas of interest.

Title Page	
Abstract	Introduction
Conclusions	References
Tables	Figures
◀	▶
◀	▶
Back	Close
Full Screen / Esc	
Printer-friendly Version	
Interactive Discussion	



Parameterizing radiative transfer

R. Sinreich et al.

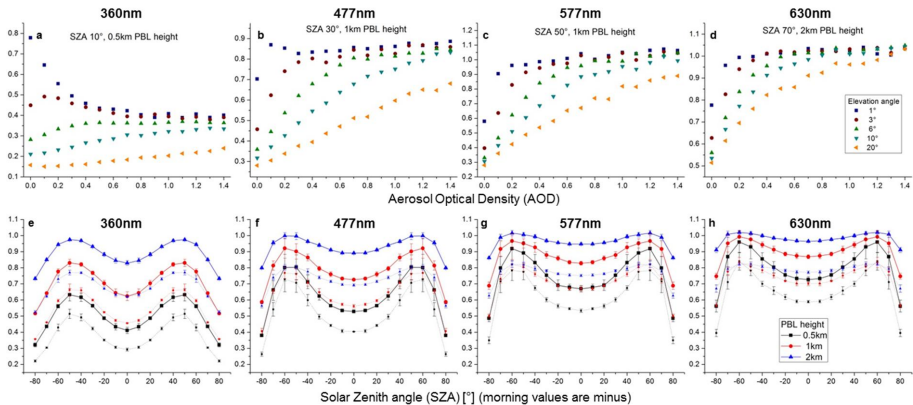


Fig. 3. (a–d): arbitrarily chosen examples for different PBL heights and SZA of calculated correction factors versus aerosol optical density for 4 different O_4 absorption bands (360 nm, 477 nm, 577 nm, 630 nm). With increasing aerosol load the correction factors form a kind of plateau; the earlier the lower the elevation angle. **(e–h):** correction factor “tooth-shaped” plots for different PBL heights (0.5 km, 1 km and 2 km) versus solar zenith angle. Thick lines indicate constant trace gas mixing ratios up to the corresponding height, thin lines represent linearly decreasing mixing ratios up to the corresponding height where it reaches zero. The aerosol profile is always a constant value up to the corresponding height. For further discussion see text.

Title Page

Abstract

Introduction

Conclusions

References

Tables

Figures

◀

▶

◀

▶

Back

Close

Full Screen / Esc

Printer-friendly Version

Interactive Discussion



Parameterizing
radiative transfer

R. Sinreich et al.

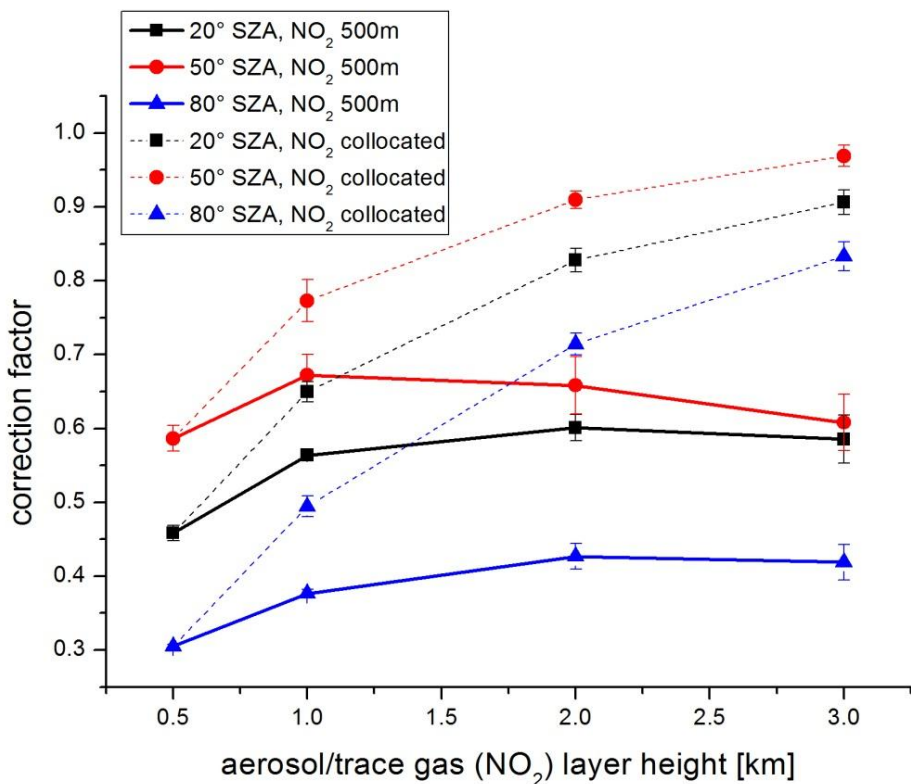


Fig. 4. Correction factors in case of a fixed NO_2 layer height of 500 m and a more extended aerosol layer up to 3000 m (thick lines) for 20°, 50° and 80° SZA for the MCMA-2006 case study. The dotted lines represent the original scenario of collocated layers.

Title Page | Abstract | Conclusions | Tables | ◀ | ◀ | Back | Full Screen / Esc

Introduction | References | Figures | ▶ | ▶ | Close | Printer-friendly Version | Interactive Discussion



**Parameterizing
radiative transfer**

R. Sinreich et al.

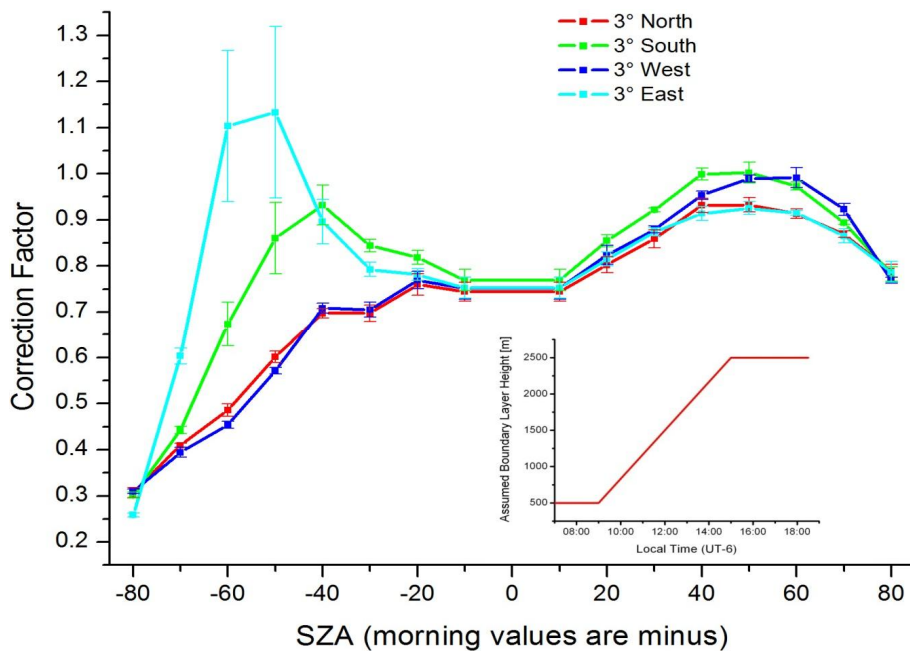


Fig. 5. Diurnal cycle of the correction factors considering SRAA and a dynamic diurnal PBL typical for Mexico City (see inset) for 4 different directions perpendicular to each other.

- [Title Page](#)
- [Abstract](#) [Introduction](#)
- [Conclusions](#) [References](#)
- [Tables](#) [Figures](#)
- [◀](#) [▶](#)
- [◀](#) [▶](#)
- [Back](#) [Close](#)
- [Full Screen / Esc](#)
- [Printer-friendly Version](#)
- [Interactive Discussion](#)



**Parameterizing
radiative transfer**

R. Sinreich et al.

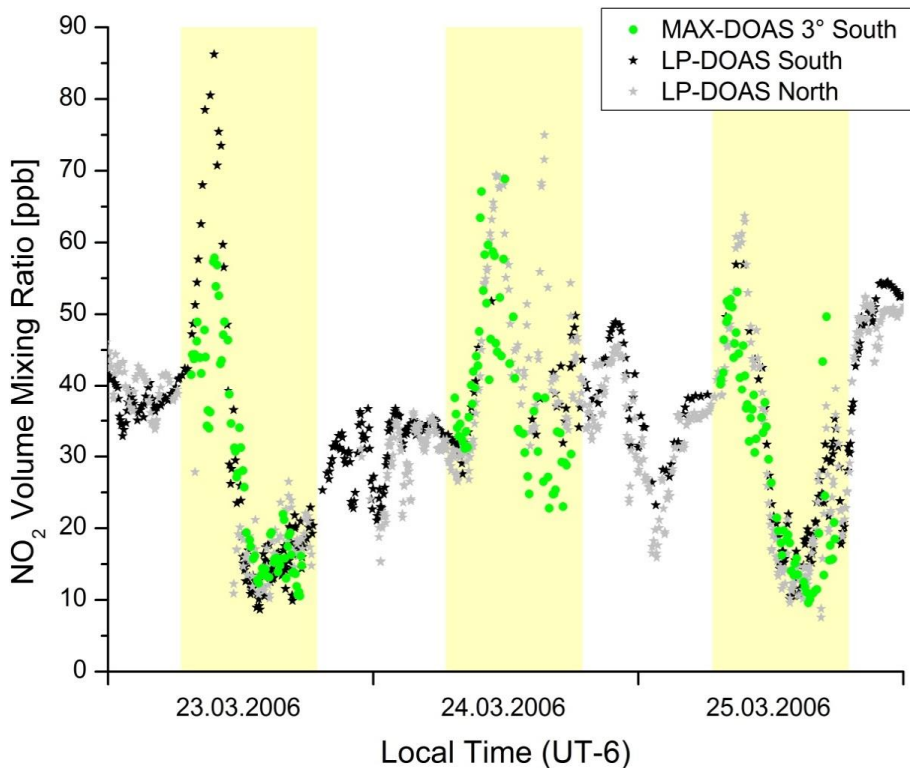


Fig. 6. Comparison of MAX-DOAS pointing South and LP-DOAS pointing South and Northwest for three arbitrary days. The light yellow background indicates daylight (SZA < 90°).

Title Page	Abstract	Introduction
Conclusions	References	
Tables	Figures	
◀	▶	
◀	▶	
Back	Close	
Full Screen / Esc		
Printer-friendly Version		
Interactive Discussion		



Parameterizing radiative transfer

R. Sinreich et al.

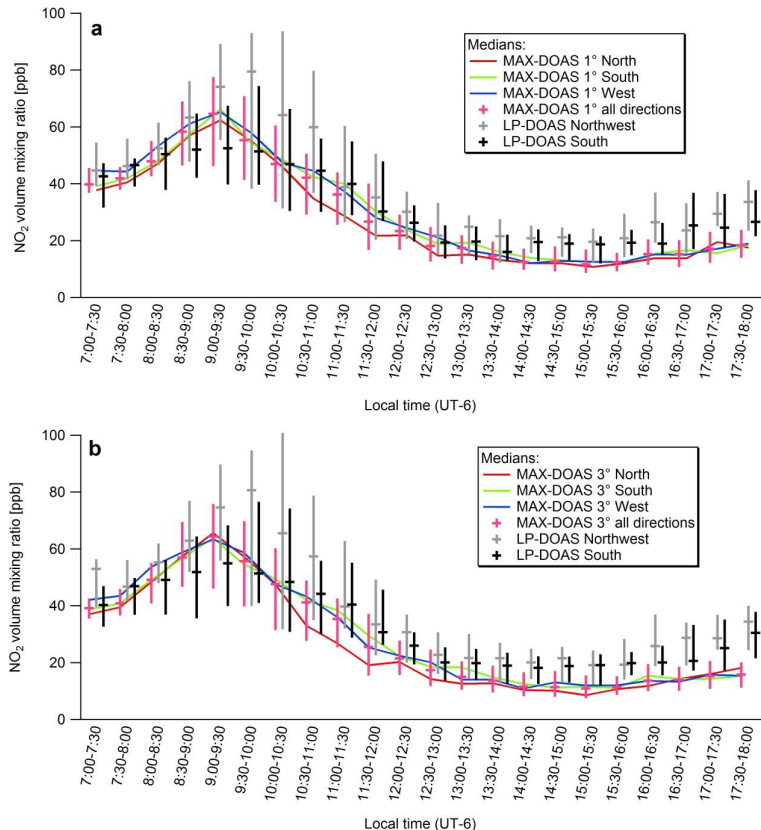


Fig. 7. Median diurnal profile (23 days) of NO₂ mixing ratios measured by MAX-DOAS in three directions and by LP-DOAS in two directions, comparing MAX-DOAS data from **(a)** 1° and **(b)** 3° elevation angle as whiskers (crosses indicate medians, vertical extensions the 25 %-tiles and 75 %-tiles of the values). The lines are the median values for the different MAX-DOAS directions.

Parameterizing radiative transfer

R. Sinreich et al.

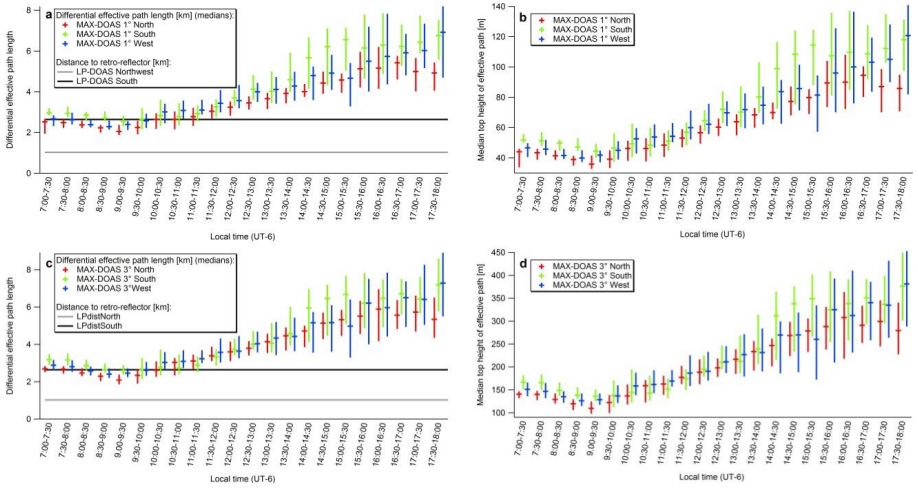


Fig. 8. Horizontal (**a, c**) and vertical (**b, d**) expansion of the MAX-DOAS measurements for 1° (**a, b**) and 3° (**c, d**) elevation angle.

- [Title Page](#)
- [Abstract](#)
- [Introduction](#)
- [Conclusions](#)
- [References](#)
- [Tables](#)
- [Figures](#)
- [◀](#)
- [▶](#)
- [◀](#)
- [▶](#)
- [Back](#)
- [Close](#)
- [Full Screen / Esc](#)
- [Printer-friendly Version](#)
- [Interactive Discussion](#)



**Parameterizing
radiative transfer**

R. Sinreich et al.

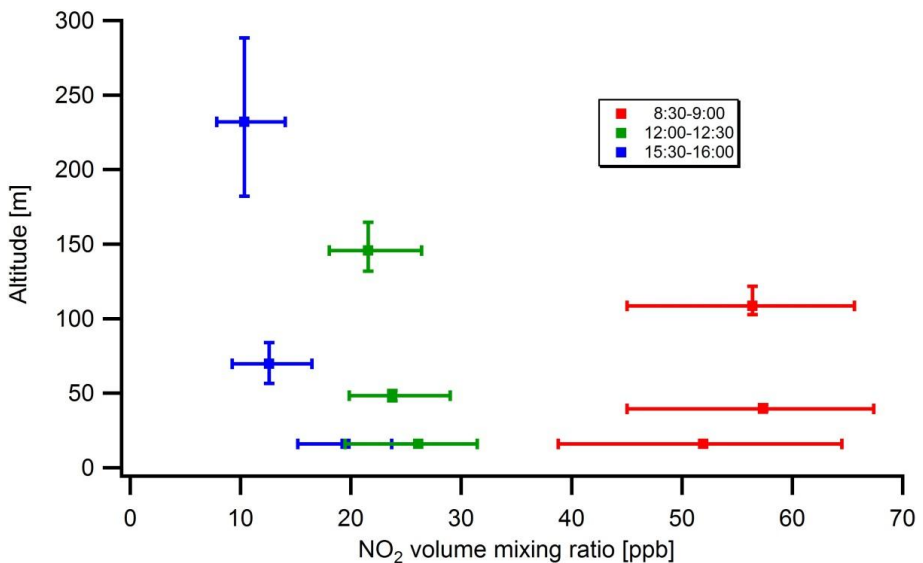


Fig. 9. NO₂ volume mixing ratio altitude profiles derived from LP-DOAS and MAX-DOAS 1° and 3° elevation angle values at a time period between 08:30 and 09:00 a.m. (red), 12:00 and 12:30 p.m. (green), and 03:30 and 04:00 p.m. (blue) in south direction.

- [Title Page](#)
- [Abstract](#) [Introduction](#)
- [Conclusions](#) [References](#)
- [Tables](#) [Figures](#)
- [◀](#) [▶](#)
- [◀](#) [▶](#)
- [Back](#) [Close](#)
- [Full Screen / Esc](#)
- [Printer-friendly Version](#)
- [Interactive Discussion](#)

